CRYSTAL GROWTH & DESIGN

Article

pubs.acs.org/crystal

Understanding the Nanostructure Formation of the Templated Two-Phase Film Growth via Hybrid Modeling

Xiao Lu,[†,‡] Boya Lai,[†,‡] Vignesh Sundar,[∥,⊥] Jian-Gang Zhu,[†,‡,§,∥] David E. Laughlin,[∥,⊥] and Jingxi Zhu*[,†,§]

[†]Sun Yat-sen University−Carnegie Mellon University Joint Institute of Engineering, School of Electronics and Information Technology, Sun Yat-sen University, Guangzhou, Guangdong, China

[‡]Department of Electrical and Computer Engineering, [∥]Data Storage Systems Center, and [⊥]Department of Materials Science and Engineering, Carnegie Mellon University, Pittsburgh, Pennsylvania 15213, United States

[§]Sun Yat-sen University−Carnegie Mellon University Shunde International Joint Research Institute, Foshan, Guangdong, China

Supporting Information

ABSTRACT: A hybrid model incorporating two methods, i.e., the Potts model Monte Carlo and the level set method, is developed to simulate the templated growth of a two-phase CoPt/SiO_2 thin film. Previously it was demonstrated experimentally that the film grown on the prefabricated template followed the pattern of the template, forming a highly ordered microstructure. The simulation in this study investigates the physical mechanism by which such film growth behavior occurs and which parameters dictate the resultant microstructure. To correctly represent the physical process, the interfacial energies between different phases and the rate of each microevent to occur were established through the simulated film deposition on a flat substrate and subsequent comparison to the experimental observations. With the established interfacial energy and rate of microevents, the resultant film microstructure grown on the templated substrate is found to strongly depend on the geometries of domes fabricated on the template. The dominant mechanism of the formation of the microstructure is shown to shift from the surface energy gradient controlled lateral diffusion in the initial stage of film growth, which formed the rudiment of the ordered microstructure, to an interfacial energy controlled process, which retained the ordered microstructure in the later stage.

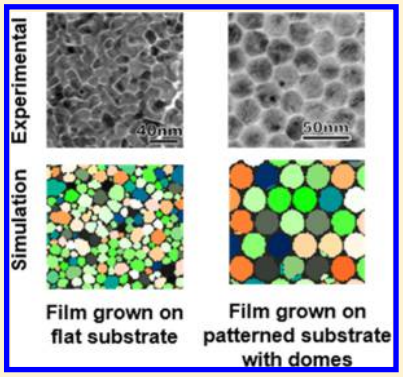

INTRODUCTION

The current commercial hard drives of computers use a composite thin film, comprised of a magnetic alloy and a nonmagnetic material, as the media for recording data. Despite the continuous increase of the storage density of hard drives for the past 50 years, the current generation commercial magnetic media is approaching its theoretical limit. The challenges that the next-generation hard drive technologies are facing, whether it is heat-assisted magnetic recording technology (HAMR), bit-patterned media technology (BPM), or microwave-assisted magnetic recording technology (MAMR), are multidimensional, which involves component design, materials selection and fabrication process design and optimization, etc.

The fabrication of the media of any of the candidate next-generation technologies becomes very challenging as the recording schemes change. One of the most important ways of improving the microstructure of magnetic media is to utilize the substrate and subsequent underlayers to control the microstructure.[1−5]

In the most desired microstructure of the media film, the nonmagnetic material must isolate the magnetic grains completely by filling their grain boundaries (GB). This is to avoid exchange coupling between the magnetic grains, which is crucial for the functioning of the media. Figure 1 shows a set of plane-view transmission electron microscopy (TEM) images comparing the effect of substrate topography on the magnetic thin film which was composed of CoPt-SiO_2.

When the substrate on which the CoPt grains grew is flat, the CoPt grains cannot be completely isolated by the partial segregation of SiO_2, as shown in Figure 1a. If the substrate topography is changed to one with nonflat dome-shaped features, the amorphous SiO_2 tend to fill the valleys between the domes where the magnetic grains grew on the tops of the domes, resulting in the microstructure shown Figure 1b. In this case, the domes were formed by sputtering Ru at a relatively high pressure. If a template is prefabricated by a process based on a nanoimprint technique, a microstructure that consists of well-isolated magnetic grains with long-range order can be achieved, as shown in Figure 1c.

In a previous study, we demonstrated a novel media film fabrication methods, in which the magnetic media film was sputtered onto a template patterned into arrays of domes.[1]

Received: August 23, 2016
Revised: December 21, 2016
Published: January 13, 2017

DOI: 10.1021/acs.cgd.6b01248
Cryst. Growth Des. 2017, 17, 1016−1027

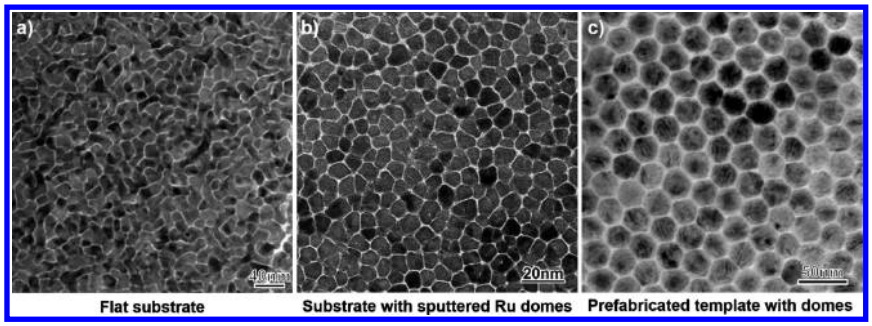

Figure 1. TEM micrographs of CoPt/am-SiO_2 magnetic media (CoPt is gray and amorphous SiO_2 is white) grown on substrate with different topographies: (a) flat Ru substrate (similar to figure in ref 9); (b) substrate with sputtered Ru domes (similar to figure in ref 10); (c) prefabricated template with domes (similar to figure in ref 11).

The templated two-phase growth method successfully controlled the microstructure of the magnetic grains, in terms of grain size, thickness of the GB segregants, etc. In particular, with the control of grain size, a distribution of 11% standard deviation was achieved.[1] However, much of the understanding of the physical mechanisms of this technique is still speculation. This study, using computational techniques, is an effort to acquire a better understanding of the physical mechanism and materials parameters behind this templated growth and the effect from substrate topography on the film as fabricated.

The complexity of the intended simulation arose from the introduction of a patterned template and the number of materials involved in the deposition, i.e., Ru as the template and on which CoPt and SiO_2 grew simultaneously during sputtering. Different hybrid models using multiscale methods have been reported which carry out the simulation of a system with multiple physical phenomena occurring on different length scales, for instance, kinetic Monte Carlo (kMC) modeling of cluster deposition considering different growth scenarios reviewed in ref 6, multiscale modeling of thin film growth by coupling the phase field method with level set method (LSM),[6,7] and the multiscale kMC method with LSM.[8]

There has also been a MC study on templated grain growth in solar thin films,[12] as well as a MC study on film growth with a scanning surface.[13] We develop a hybrid method in this work for modeling the templated two-phase growth of the magnetic media thin film. By coupling the scanning surface Monte Carlo (MC) method with the level set method (LSM), a three-dimensional model was built, within which the deposition process of the CoPt-SiO_2 magnetic media could be simulated.

FRAMEWORK OF THE SIMULATION

Monte Carlo Simulation. *Potts Model.* The MC simulation of the current study is based on the Potts model,[14] originally derived from the Ising model[15] for the computation of magnetization. The Potts MC was later extended to the study of grain growth driven by GB curvature and its microstructural evolution.[12] The main considerations of the Potts model are the different types of energies in the system and the probability of certain events occurring driven by the minimization of the total energy of the system. The Potts model MC can be used to simulate thin film deposition because it is essentially a sequence of equilibration of each arriving atoms and hence is also a process related to energy minimization.[14] Hence, this work studies the interplay between different energies and their effects on the resultant microstructure, and was conducted in a three-dimensional (3D) scheme to fully present the final microstructure.

The 3D space in this model is discretized into cubes, or voxels, with the voxel edge length being 0.8 nm. A random number is assigned to each voxel representing different components in the system at the beginning, but will change later driven by the minimization of the total system energy, and the probability of these changes are subject to the metropolis algorithm.[16] As a result, clusters of voxels with the same number will form and they are considered as grains of the phases.

The total energy or the Hamiltonian of the system to be minimized through the simulation can be expressed as eq 1:

$$H = \frac{1}{2}\sum_{i=1}^{N}\sum_{j=1}^{NN}\gamma_{Q_iQ_j}(1-\delta_{Q_iQ_j}) \tag{1}$$

where Q_i and Q_j denote the species on site i and its neighbor j, termed as phase ID in this paper; $\gamma_{Q_iQ_j}$ is the interfacial energy between sites i and j, where this interface can be a GB or an interface separating the two species. NN is the number of the neighbors of one voxel and is taken to be 26 for a 3D cubic grid considering up to the third neighbor. δ is the Kronecker delta function ($\delta_{mn} = 1$ if $m = n$; $\delta_{mn} = 0$ otherwise).

Driven by the total system energy minimization, two events could potentially happen in the system:

(1) The voxel may reorient (crystallographically).

(2) The voxels may exchange sites with other voxels of a different species (as in a multimaterials system).

The Metropolis algorithm[16] determines the probability of each event, namely, the Metropolis probability P shown in eq 2, and compares it to a randomly generated number P_{rand}, where $P_{rand} \in (0,1)$. An event is accepted if $P > P_{rand}$, and rejected otherwise.

$$P = \begin{cases} \dfrac{M}{M_{max}}\exp\left(\dfrac{-\Delta E}{kT}\right), \text{ if } \Delta E \le 0 \\ \dfrac{M}{M_{max}}, \text{ otherwise} \end{cases} \tag{2}$$

where ΔE is the energy change, k is the Boltzman's constant, and T is the temperature. M is essentially related to the "rate" at which each event occurs. M_{max} represents the maximum mobility of surface diffusion.

Scanning Surface Method. The conventional Potts model MC simulation can only be applied to a predefined fixed volume filled with voxels. This does not apply to film growth scenarios, where the volume of the system changes continuously. Without resorting to more complicated computational methods suitable for dynamic systems, the scanning surface method stood out as a straightforward and computational efficient method, developed specifically to simulate film growth alongside Potts MC.[13]

DOI: 10.1021/acs.cgd.6b01248
Cryst. Growth Des. 2017, 17, 1016−1027

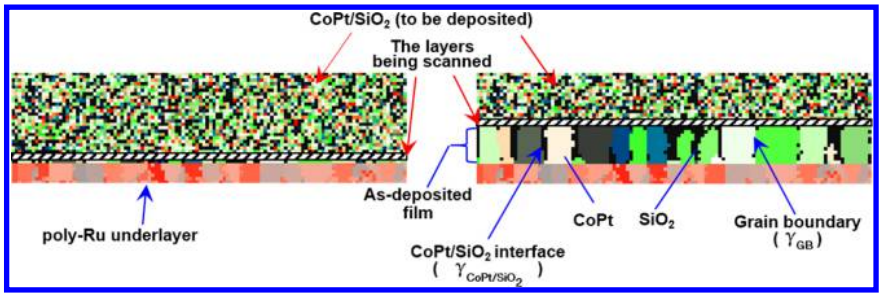

Figure 2. Schematic drawing of the scanning surface MC method: (left) initial state of the simulated film growth; (right) intermediate state during simulated film growth (γ indicates the interfacial energy involved).

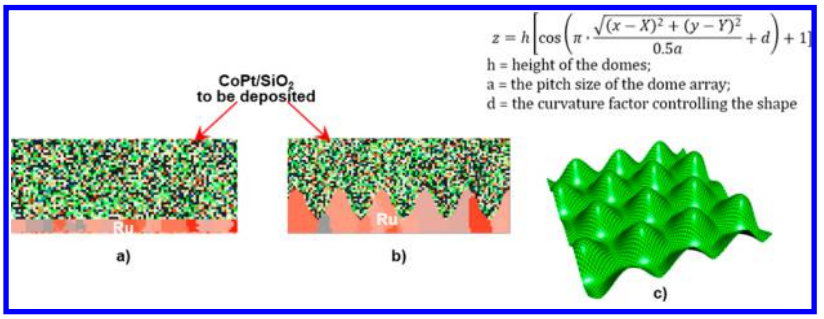

Figure 3. Schematic drawing of $CoPt/SiO_2$ deposited onto different substrates: (a) flat substrate, (b) templated substrate with prefabricated domes; (c) 3D visualization of a section of the dome array on the template.

This process is shown in the 2D cross-sectional view in Figure 2 for the magnetic media film in this study. In the initially predefined volume, the Ru substrate is the bottom immobile layer. The two-phase film to be deposited is a completely randomized mixture of CoPt and SiO_2 represented by the mixture of voxels with different colors in Figure 2. The volume fraction of SiO_2 was set to 25% following the experimental study in ref 1 and was also used throughout the entire study. The simulation started with the first to-be-deposited layer of voxels activated and equilibrate through a certain number of MCSs. Next, the scanning surface moved up one layer and activated the next layer of voxels, while deactivating the first layer. Note that the SiO_2 vol % was fixed to be 25% within every layer of voxels that was activated. This procedure was repeated until reaching the desired film thickness. In this way, the simulation of a non-isovolumetric film growth process was achieved by using an isovolumetric method that sequentially simulates the equilibration of a very thin layer of the film deposited.

Materials Components of the Thin Film Systems. Two substrates were used in this study: a flat substrate and a templated substrate with dome-like features as shown in Figure 3, panels a and b, respectively. Because the film microstructure of the former have been studied quite thoroughly and with abundant experimental work available for comparison, such as in Figure 1a, the parameter determination and validation was carried out using a flat substrate. Once the appropriate simulation parameters were chosen, the mechanistic investigation of microstructure formation under the influence of the templated substrate could be performed.

Considering the epitaxial relationship between Ru(0002) and CoPt(0002), it is highly favored energetically for CoPt grains to grow with their *c*-axis perpendicular to the plane of the film.[17] Hence, integers were assigned to represent different orientations of the CoPt grains with fiber texture whose *c*-axis are aligned in the perpendicular direction while having different in-plane orientations.

Experimentally, the templated substrate with dome arrays was fabricated with a Pt film using block copolymer self-assembly. Before the magnetic media film (CoPt + SiO_2) was sputtered onto the template, a thin Ru layer (~5 nm thick) was deposited onto the template, which was critical for the texturing of the CoPt grains.

In this work, to simplify the building of the geometric model for the templated film, we omitted the Pt layer present in the experimental fabrication and built the domes entirely out of Ru. The dome shape was approximated as a periodic cosine function, which closely resembled the experimentally fabricated domes on the template in ref 1. The domes on the template were organized in a hexagonal array, as shown in Figure 3c. The pitch size of the dome array was set to be 16 nm here, also following the work in ref 1. The shape of the domes could be changed for various simulations by altering the geometric parameters, which are also controllable in experimental fabrication processes.

Energy Terms. As mentioned in the previous section, the main considerations of the Potts model are the different types of energies in the system and the probability of certain events occurring driven by the minimization of the total energy of the system. The resultant overall microstructure of the media film will largely depend on the interplay between different energy terms in this multimaterial system. Table 1 tabulates all the energy terms considered in our model and their notations, as well as generalized notations. Thus, eq 1 can be rewritten as

$$H = \frac{1}{2}\Big[\gamma_{\mathrm{CoPt/SiO_2}} \sum_{i=1}^{N_{\mathrm{SiO_2}}} \sum_{j=1}^{NN} (1 - \delta_{Q_iQ_j}) + \gamma_{\mathrm{GB}} \sum_{i=1}^{N_{\mathrm{CoPt}}} \sum_{j=1}^{NN} (1 - \delta_{G_iG_j}) + \gamma_{\mathrm{epi}} \cdot \sum_{i=1}^{N_{\mathrm{Ru}}} \sum_{j=1}^{NN} (1 - \delta_{U_iU_j}) + \sum_{i=1}^{N^S} E_i^s\Big] \quad (3)$$

DOI: 10.1021/acs.cgd.6b01248
Cryst. Growth Des. 2017, 17, 1016−1027

Table 1. Interfaces Present in the Current Multi-Material System and Their Corresponding Energy Terms Considered in Our Model

interface	types of interface	notations	generalized notations	description
CoPt/CoPt	grain boundary	$\gamma_{CoPt/CoPt}$	γ_{GB}	GB energy of CoPt grains
CoPt/Ru	epitaxial interface	$\gamma_{CoPt/Ru}$	γ_{epi}	denoted as γ_{epi} hereafter due to the epitaxial interface between CoPt and Ru
CoPt/SiO_2	general interface	γ_{CoPt/SiO_2}	γ_{CoPt/SiO_2}	γ_{CoPt/SiO_2} and γ_{Ru/SiO_2} were considered equal for simplicity and generalized as γ_{CoPt/SiO_2}
Ru/SiO_2	general interface	γ_{Ru/SiO_2}	γ_{CoPt/SiO_2}	
CoPt/vacuum	surface	γ_{CoPt}	E^S_{CoPt}	calculated from the broken bonds model, to be implemented in the mobility considerations
SiO_2/vacuum	surface	γ_{SiO_2}	$E^S_{SiO_2}$	

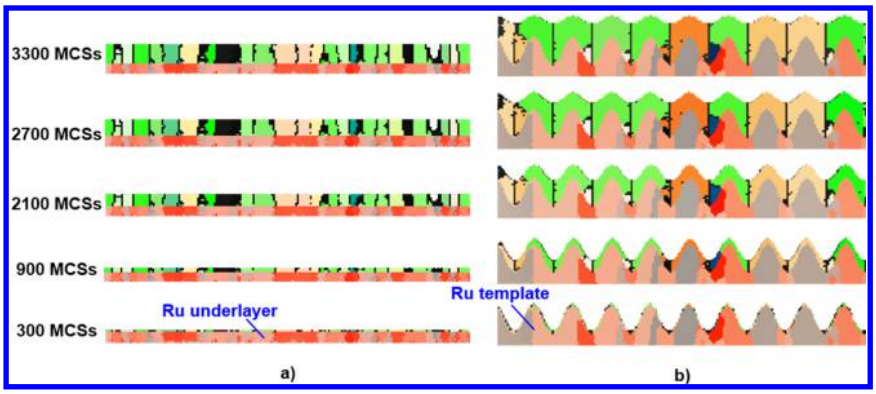

Figure 4. Cross-sectional snapshot of Monte Carlo simulated two-phase film growth on polycrystalline Ru (a) flat substrate; and (b) templated substrate with aspect ratio = 0.8 and cone-like domes (MCS = Monte Carlo steps).

where N_{SiO_2}, N_{CoPt}, N_{Ru}, and N^S are the number of voxels occupied by SiO_2, CoPt, and Ru, and the number of voxels on the surface respectively; Q_i or Q_j denotes the materials occupying the site i or j, showing if site i or j is occupied by SiO_2 or not; G_i or G_j represents the orientation of the voxels occupied by CoPt; U_i or U_j denotes the materials occupying the site i or j, showing if site i or j is occupied by Ru or not; E^s_i is the surface energy of material i,

The voxel lattice temperature in the Potts model MC simulation influences the probability of each event exponentially. An optimal lattice temperature allows the system to overcome the voxel lattice anisotropy,[18] without introducing too much randomness into the results. In this study, the lattice temperature was optimized and expressed as kT, which satisfies $\gamma_{epi}/kT = 1.2$. (γ_{epi} is the smallest energy term of the simulation.)

Mobility Considerations. The mobility term in the Potts model MC, expressed as M in eq 2, is essentially related to the "rate" at which each event occurs, either an exchange event (otherwise dubbed surface diffusion) or a reorientation event. The implementation of mobility enables the scaling of the rates of different events within the same time length scale, i.e., one Monte Carlo step, and helps explain the kinetics of the overall film growth process. M stands for atomic mobility for surface diffusion and the rate of reorientation for reorientation events, similar to the GB migration rate[19] and can be expressed by eq 4. Accordingly, the maximum mobility is written as eq 5.

$$M = M_0 \exp\left(\frac{-E^{Act}}{kT}\right) \tag{4}$$

$$M_{max} = M_0 \exp\left(\frac{-E^{Act}_{min}}{kT}\right) \tag{5}$$

However, the activation energies, E^{Act}, for two types of events to occur are different.[20] M_0 is a prefactor related to the atomic vibration frequency. In this study, we estimated E^{Act} following the transition state theory,[21,22] which related the activation energy with the change of the bonds formed between a voxel with its neighbors before and after the occurrence of diffusion, while the bonding energies between different types of materials were calculated from the broken bond theory. Mathematical details of activation energies are described in Supporting Information S1.

Level Set Method and Its Coupling with Scanning Surface MC Method. Unlike films grown on a flat substrate, the film growth in this study starts off from a nonflat surface, i.e., a patterned template with a dome morphology. Thus, the planar surface used for scanning in the ref 12 cannot be applied without modification. Also, the film surface topography evolves as the film thickens. Therefore, the surface to be scanned here must be a dynamically evolving 3D surface as a function of time. The LSM has been demonstrated to successfully simulate the evolution of a crystal growth problem[23−25] and was incorporated in this model order to obtain an accurate mathematical description of the undulated surface of CoPt−SiO_2 film.

The CoPt-SiO_2 film surface is the one to be traced during the deposition and can be represented by a 2D moving hypersurface: Γ. In LSM simulation, a level set value $\phi(x,y,z)$ is distributed within the space being simulated, which stands for the distance between the location (x,y,z) and the hypersurface, and could indicate whether this point is on the hypersurface Γ with $\phi = 0$, or not with $\phi \neq 0$. As time evolves, with the velocity field $V(\vec{x})$ being well-defined with respect to the growth rate of film, the level set value of a point, or the distance between each point and the surface, changes following the level set function expressed below:[26]

$$\frac{\partial \phi}{\partial t} + V(\vec{x})\cdot\nabla\phi = 0 \tag{6}$$

It needs to be noted that in this approach, even though $V(\vec{x})$ is the velocity of each location point, only those points close to the

DOI: 10.1021/acs.cgd.6b01248
Cryst. Growth Des. 2017, 17, 1016−1027

surface could change the morphology of the surface during evolution.[27,28] Numerical methods were then applied to solve this equation by the discretization of the simulated space into grids. More details of the mathematical derivations of LSM in this simulation can be found in ref 29.

By substituting the planar surface in the scanning surface method by the 3D dynamic surface obtained with LSM, the scanning surface MC method can now be extended to the templated film growth. The entire simulation consisted of a large number of mini-MC processes, during each of which the film microstructure is allowed to equilibrate with the surface provided by LSM.

This hybrid simulation method is essential for us to study the influence of substrate geometry, which was not necessarily a flat plane, on film growth.

RESULTS AND DISCUSSION

Cross-Sectional Visualization of the Film Growth. Figure 4 shows the cross-sectional snapshots of the simulated two-phase film growth on polycrystalline Ru flat substrate. In general, different colors represent different crystallographic orientations. Polycrystalline Ru with the [0002] fiber texture was implemented for both flat and templated substrates, and the different Ru grains were represented by different shades of red. Other colors, excluding black, were assigned for CoPt grains. The black color represents amorphous SiO_2 in the simulation. A grain-to-grain matching between CoPt and Ru grains is observed due to the small mismatch between Ru(0002) and CoPt(0002). In addition, SiO_2, colored as black, segregates to the grain boundaries and partially fills them.

How the Resultant Microstructure Changes. *Interfacial Energies between Different Species.* The functionality of the current PMR media relies on the isolated magnetic grains separated by a GB segregant to prevent exchange coupling between neighboring grains. This requires the use of two immiscible materials to fabricate the media film, and the interfacial energies between them and the underlayer play a crucial role in the formation of the microstructure. Hence, first we investigated how the resultant microstructure changed with the interfacial energy terms in this simulation, i.e., the γ_{epi},γ_{CoPt/SiO_2} and γ_{GB} terms. To avoid interference from other effects, a flat substrate was used, and only interfacial energy terms were considered. The scanning surface MC scheme was applied and two voxel layers were activated during each scan, allowing diffusion to occur in both the in-plane and out-of-plane directions.

To present the results in a quantitative manner, the GB coverage (in percentage) by SiO_2 was used to reveal the effects of the energy terms on the resultant film microstructure for the reason stated above and was defined as the percentage out of the total GB length that was covered by SiO_2. The total volume fraction of SiO_2 in the composite film was fixed at 25%.

Referring to Table 1, γ_{GB}, γ_{CoPt/SiO_2}, and γ_{epi} are the terms influential on the microstructure through energy minimization process, if no other effects were taken into consideration.

The interface between CoPt and Ru(0002) planes, with lattice mismatch less than 5%,[30] is essentially considered as epitaxial, and the corresponding interfacial energy γ_{epi} was the lowest in this model compared to that of all the other incoherent interfaces.

Because the CoPt/SiO_2 interface remained largely unexplored due to its complexity, it was simplified here as an isotropic interface irrespective of all the possible atomic bonding between four types of atoms. The ratio between γ_{epi} and the interfacial energy γ_{CoPt/SiO_2} was fixed ($\gamma_{CoPt/SiO_2} = 5\cdot\gamma_{epi}$) to represent the immiscibility between SiO_2 and Ru. The details of the optimization of the $\gamma_{CoPt/SiO_2}/\gamma_{epi}$ ratio through maximizing the GB coverage can be found in Supporting Information S2. The GB energy γ_{GB} was also treated as isotropic, irrespective of the GB characters.

Figure 5 shows how the microstructure changes with the changing of the ratio between γ_{GB} and γ_{CoPt/SiO_2}, between

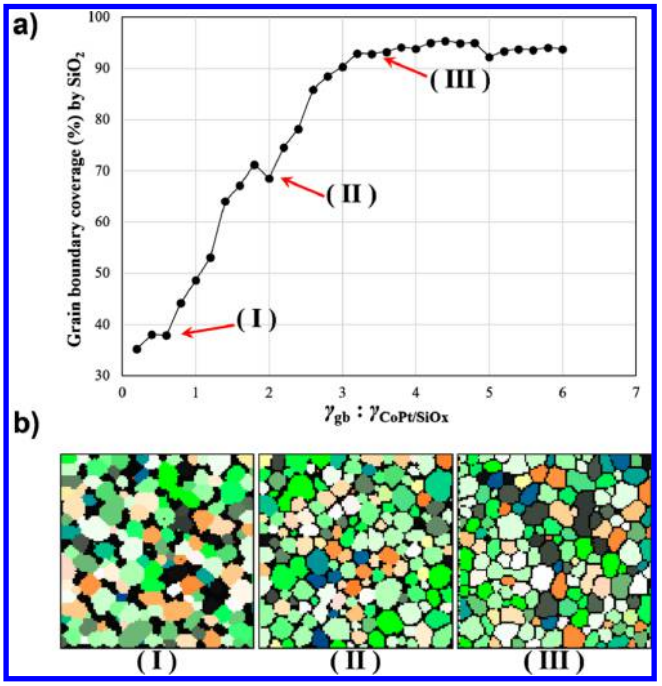

Figure 5. Influence of interfacial energy on two phase film grown on flat substrate: (a) change of GB coverage by SiO_2 in percentage and (b) corresponding microstructures.

0.1 and 6. The GB coverage of the resultant film microstructure was plotted against the ratio of $\gamma_{GB}/\gamma_{CoPt/SiO_2}$, as shown in Figure 5a. Simulated microstructures at specific energy ratios are shown in Figure 5b.

As can be observed in Figure 5b(I), for small energy ratios ($\gamma_{GB}/\gamma_{CoPt/SiO_2} = 0.2$), adjacent CoPt grains were poorly segregated by SiO_2, having low SiO_2 coverage in the grain boundaries and SiO_2 (in black color) coalesced into small clusters at triple-junctions of the CoPt grains. This was because when γ_{CoPt/SiO_2} became comparable to γ_{GB}, there was no particular advantage energetically to have higher GB coverage, which should be the low energy state favored under energy minimization.

When $\gamma_{GB}/\gamma_{CoPt/SiO_2}$ increased beyond 1, i.e., the formation of GBs became less energetically favored, SiO_2 started to cover the GBs to minimize total energy of the system, which meant that grain boundaries became favored sites for SiO_2 to occupy. Figure 5b(II) shows a microstructure with GBs partially filled by SiO_2. In this case, $\gamma_{GB}/\gamma_{CoPt/SiO_2} = 2$. CoPt grains could be considered as completely isolated by SiO_2 when $\gamma_{GB}/\gamma_{CoPt/SiO_2} = 3.2$ in this model, which was indicated by a GB coverage of ~93% at (III), also see Figure 5b (III). As $\gamma_{GB}/\gamma_{CoPt/SiO_2}$ continued to increase, this full isolation of adjacent CoPt grains

DOI: 10.1021/acs.cgd.6b01248
Cryst. Growth Des. 2017, 17, 1016−1027

by SiO_2 remained (shown as a plateau in the GB coverage curve). Also, a roughly exponential increase of GB coverage as a function of the energy ratio could be noted in the range swept, which may be caused by the exponential dependence of the probability of events occurring on the energy change in MC method.

From the results described above, a strong dependence of microstructure and interfacial energy could be observed which extended the simulations from 2D carried out in refs 31 and 32, to a 3D scheme. By comparing the simulation results to experimental film microstructure grown on flat substrates in Figure 1a, the former matched the latter the best at $\gamma_{GB}/\gamma_{CoPt/SiO_2} = 2$, and therefore the relative ratio between the three generalized interfacial energy terms could be determined for the simulation of the templated growth as $\gamma_{epi}/\gamma_{CoPt/SiO_2}/\gamma_{GB} = 1{:}5{:}10$ (with predefined $\gamma_{CoPt/SiO_2} = 5{\cdot}\gamma_{epi}$ in S2). The semiequilibrium state of the system was correctly represented by the film microstructure in which CoPt grains were partially isolated by SiO_2 on the flat substrate and underlayer.

Mobility in Relation to the Surface Energies of the Two Phases. To properly evaluate the effects of mobility on the film microstructure, one must determine an appropriate interfacial energy ratio $\gamma_{GB}/\gamma_{CoPt/SiO_2}$, at which such effects would be clearly observable and not be influenced by anything else other than mobility. Therefore, a ratio of $\gamma_{GB}/\gamma_{CoPt/SiO_2} = 3.2{:}1$ was chosen, at which the GB coverage $\approx$ 100% and the variation in GB coverage due to mobility change could be well represented.

As expressed in eq 4, the rate of each microevent to occur is dependent on the activation energy, which is calculated from bonding energy between different species according to the transition state theory, and referring to the broken bond model, bonding energy can be expressed in terms of surface energy. The details of activation energy can be found in Supporting Information S1.

A similar simplification, as the one made for γ_{CoPt/SiO_2}, was applied here which took E^S_{CoPt} to be isotropic even though, based on broken-bond model, the calculation from density function theory indicates that the surface energy of CoPt would vary on different facets.[33] The value of surface energy for CoPt used in this model is 2.2 J/m^2 which, as discussed in ref 34, is computed using quenched molecular dynamic method and is on the same order of magnitude of the Co and Pt surface energy measured in experiment[35] and calculated using broken bond model.[36] This isotropic consideration of surface energy, and the hcp CoPt grain boundary energy, is qualitatively accurate. However, to be quantitatively precise, CSL model for CoPt grain boundary energy and facet-dependent surface energy could be implemented for accuracy improvement but is not the focus of this study. The computed theoretical value for $E^S_{SiO_2}$ for amorphous SiO_2 is ~1.5 J/m^2, achieved through computation using broken bond model.[37] This value was expressed as a ratio over the real value of γ_{epi}, i.e., $E^S_{SiO_2}/\gamma_{epi} = 15{:}1$, in this result and the following simulations. Using the same strategy as the evaluation on the energy terms, with $\gamma_{GB}/\gamma_{CoPt/SiO_2} = 3.2{:}1$, the effect of different rates, i.e., the mobility for diffusion and the rate of reorientation, can be investigated by sweeping the E^S_{CoPt}/γ_{epi} ratio (superscript "S" stands for surface), in which the surface energy of CoPt, E^S_{CoPt} is an important energy term for diffusive mobility. Figure 6 shows the resultant microstructures varying as a function of the ratio between $E^S_{SiO_2}$ and γ_{epi} in terms of the GB coverage.

When E^S_{CoPt} is small, the bonding of CoPt/CoPt was the weakest among the three bonds: $E^{bonding}_{CoPt/CoPt} < E^{bonding}_{CoPt/SiO_2} < E^{bonding}_{SiO_2/SiO_2}$ (details in Supporting Information S1). In this case, SiO_2 with stronger bonds had lower mobility, and the rate of SiO_2 diffusion was smaller compared to the diffusion of CoPt. Therefore, the process of total energy minimization was hindered by the limited mobility of SiO_2, and the system could not move further toward the final semiequilibrium state achieved in the previous section. As a result, SiO_2 formed small clusters to reach a local energy minimum state with its limited mobility, whereas the CoPt grains could still coarsen (shown in Figure 6b(I)). Also, for the

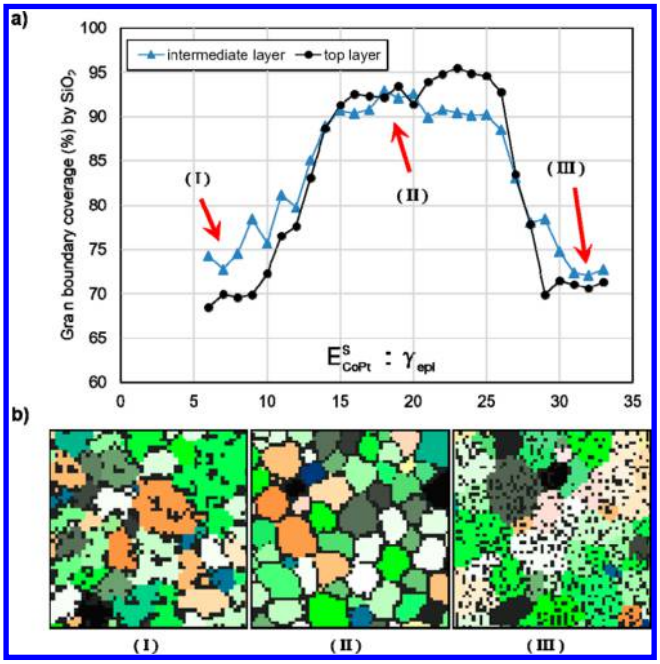

Figure 6. Influence of mobility as a result of changing surface energy on CoPt + SiO_2 film grown on a flat substrate: (a) change of GB coverage by SiO_2 in percentage and (b) corresponding microstructures.

intermediate voxel layers (ones that were above the substrate and below the surface layer of the film), their average GB coverage was noticeably higher than that of the surface layer. The reason is that E^S_{CoPt} being the lowest energy led to CoPt enriching on the surface, while the less mobile SiO_2 segregates within the film. This has not been experimentally observed.

When $E^{bonding}_{CoPt/SiO_2} < E^{bonding}_{SiO_2/SiO_2} < E^{bonding}_{CoPt/CoPt}$, the bonding of CoPt/$SiO_2$ became the weakest. Also, with CoPt/CoPt bonds being stronger than SiO_2/SiO_2 bonds, CoPt is more likely to bond with the neighboring voxels of the same material, making the mobility of CoPt lower than that of SiO_2 at CoPt/SiO_2 interface. In other words, this maximizes the mobility of SiO_2 at the CoPt/SiO_2 interface. Thus, comparing Figure 6b(II) and Figure 5b(II), SiO_2 was able to cover the GB completely with increased mobility and enabled the system to equilibrate globally. Moreover, regardless of which species had higher surface energy, the SiO_2 diffusion from within the film to the film surface was still limited by the oxide−oxide bonds formed in the GB beneath the surface. Hence, the diffusion rates for both metal and oxide in the film were limited, which was in fact a reasonable scenario for film deposition carried out under room temperature or water-cooled substrate, and the system was constrained to a semiequilibrium state determined by the effect of interfacial energy.

DOI: 10.1021/acs.cgd.6b01248
Cryst. Growth Des. 2017, 17, 1016−1027

When E^{S}_{CoPt} was further increased, the SiO_2/SiO_2 bonding became the weakest. Even though a SiO_2/SiO_2 neighboring pair would have been the lowest energy state for SiO_2, this state could not be sustained for the amount of MC steps given in our simulation for each scan. As a result, SiO_2 dispersed within the film due to its highly increased mobility. The corresponding microstructure is shown in Figure 6b(III). The low coverage in this regime was representative of the mixed microstructure even though the equilibrium state of the system was set for SiO_2 to completely isolate the adjacent CoPt grains.

Hence, in order for the system to reach the minimized energy state within a reasonable amount of time, the mobilities of the components were crucial. Again, by comparing the simulation results with the rate of each event taken into account to the experimental film microstructure grown on flat substrates, the surface energy of CoPt E^{S}_{CoPt} fell within regime (II) in Figure 6a. Nevertheless, if materials existed whose surface energy satisfied that specified in regime I and III, the microstructures shown in Figure 6b(I) and (III) would potentially be realized by changing the components of the composite film.

Template Geometry. The simulation shown in Figures 5 and 6 were carried out to understand how interfacial energy terms and mobility of the species affect the resultant film microstructure formed on a flat substrate. With these results, it was also possible for us to determine a set of parameters with which a simulated microstructure that matched very well to the experimental ones could be produced. This set of parameters closely represented the properties of the materials in the film system as well as reflecting some aspects of the experimental deposition conditions commonly used in fabricating this type of media film. With these parameters, it is now possible to investigate the effect from the templated substrate, its geometry in particular, on the resultant film microstructure.

Moreover, for a nonplanar substrate, considerations of how the surface energy would change due to local geometry (or curvature relative to a flat surface) must be included in the simulation, namely, the Mullin's theory[38] of surface energy and expressed as eq 7.

$$\mu_s = \mu_0 + \gamma_S \Omega \kappa \tag{7}$$

where μ_s is the chemical potential, μ_0 is the chemical potential of a flat substrate, γ_s is the surface energy per area (J/m^2), Ω is the atomic volume, and κ is the mean local curvature. This means, if the chemical potential of a flat substrate is the same everywhere, merely by having a nonzero local curvature introduces an increased potential energy to the surface. If such curvature varies continuously across the surface such that a surface energy gradient as well as a chemical potential gradient are effectively introduced and thus becomes the driving force for surface diffusion to occur. The domes on the template in our simulation have done just that. In other words, under the chemical potential gradient introduced by the domes, the surface diffusion on a patterned substrate will occur and following the direction of the curvature gradient. The following results were obtained with the optimized model by varying the geometry of the Ru domes on the template during the simulation of the film growth.

1. Single Crystal Substrate Simulation. First, a simple simulation with patterned single crystal Ru template was performed, as shown in Figure 7. By using a single crystal, the energy term γ_{GB} was eliminated, which simplified the clarification of the interplay between the interfacial energy and mobility of different species.

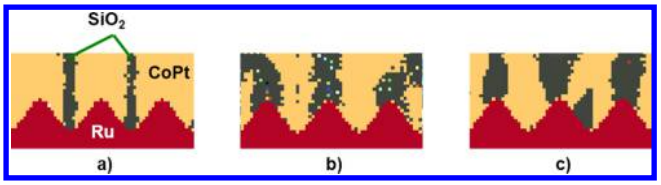

Figure 7. Cross-sectional snapshot of two phase film growth on patterned single crystalline substrate when (a) CoPt and SiO_2 both having physical mobility and surface energy taking the Mullin's theory into account; (b) both CoPt and oxide have maximum mobility; (c) without taking the Mullin's theory into account.

In Figure 7, the CoPt grains grew epitaxially on the single crystalline Ru template. The microstructural difference between Figure 7, panels a and b stems solely from the mobility. If CoPt and SiO_2 diffused with the mobilities as determined in regime II in Figure 6a, the mobile species, SiO_2, would diffuse following the curvature gradient and start growing from the bottom of the valley, as shown in Figure 7a, and the whole system would reach a low energy state S_1 with total energy being reduced by SiO_2 filling the valley equaling to ΔE_1. Whereas in the case of Figure 7b, if both CoPt and SiO_2 artificially acquired the same maximum mobility, the species with higher surface energy, i.e., CoPt as determined previously, would diffuse into the valley to minimize the total energy, and the system would reach a state S_2 with total energy being reduced by ΔE_2. Since the process with bigger energy reduction is favored in MC simulation, with $\Delta E_1 > \Delta E_2$, state S_1 is favored than state S_2, so that it is more energetically favored for CoPt to fill the valleys, being state S_1. However, because of the limited mobility of CoPt, the probability of overcoming the energy barrier between S_1 and S_2 was low, and the transition from S_1 to S_2 was inhibited. Thus, Figure 7a shows the case with mobile species SiO_2 diffusing along the chemical potential gradient from the top of the dome into the valley.

A comparison between Figure 7, panels a and c shows the microstructure difference with and without Mullin's theory considered in our model, respectively. In case c, SiO_2 would coalesce and form clusters irrespective of the topography of the domes if Mullin's theory of surface energy is not considered. In other words, there lacked a driving force for the SiO_2 to diffuse to the bottom of the valley. Detailed diffusion behavior is discussed in Supporting Information S3 as a quantitative proof for the different motion steps for CoPt and SiO_2.

2. Domes of Different Aspect Ratios (AR). In this section and the one that follows, results on the effect from the geometric aspects of the template, i.e., the dome morphology in particular, will be presented and discussed in light of the Mullin's theory. This enables us to quantify the modification of surface energy due to local geometry and introduces an extra driving force for surface diffusion. In the simulation of this regard, we varied the dome geometry quantitatively in terms of aspect ratio (defined as dome height divided by the pitch size) and shape. Other energy related parameters that were determined in the previous sections were kept the same. The grain size, its distribution, and the grain center-to-center distance (and its distribution) will be used for quantitative evaluation of the resultant microstructure. If the template was able to guide the CoPt grain growth, then the most ideal case would give a grain center-to-center distance equal to the pitch size of the dome array, and accordingly, the average grain size would be just slightly smaller than the dome array pitch size with a very narrow grain size distribution (with SiO_2 filling the GBs). Also, to be realistic, the grain size of the Ru template were kept smaller than the pitch size a.

DOI: 10.1021/acs.cgd.6b01248
Cryst. Growth Des. 2017, 17, 1016−1027

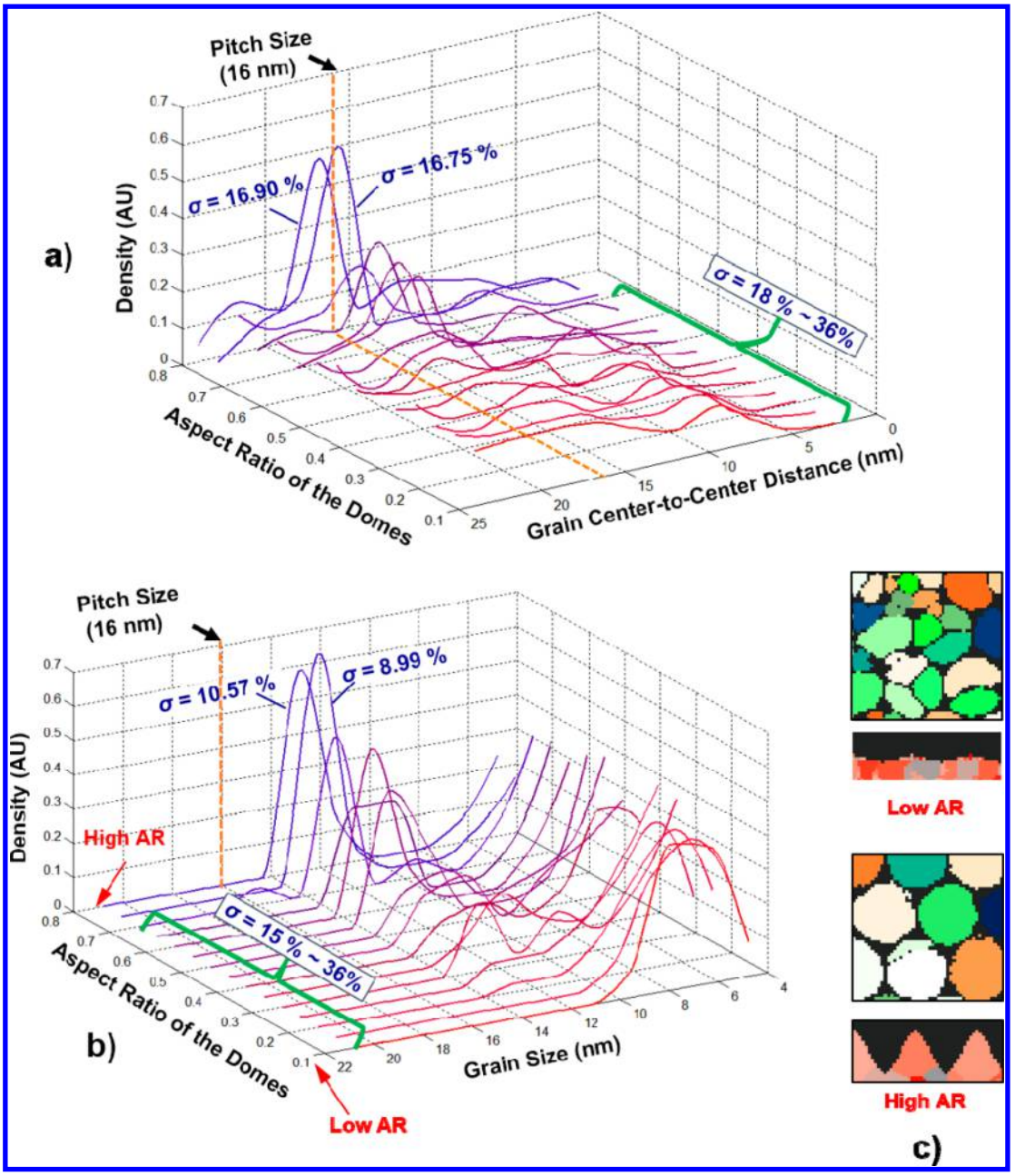

Figure 8. Effect of the aspect ratio of the domes on the two-phase growth and the resultant microstructure (a) grain center-to-center distance and its distribution σ; (b) grain size and its distribution σ; (c) plane view of as-simulated films with different dome aspect ratio (shown below each plane view of domes).

As shown in Figure 8a, the grain center-to-center distance becomes more and more narrowly distributed ($\sigma \approx 16\%$) around the dome pitch size (i.e., 16 nm) as the dome aspect ratio increases, indicating that a sufficiently large aspect ratio is required for the template to effectively guide the two-phase growth of the film. It can also be speculated that a critical aspect ratio exists, 0.7 in our simulation, at which guided two-phase growth would become possible. Figure 8b shows that as the aspect ratio of the domes increases up to 0.7, the grain size increases in general, up to slightly less than 14 nm, while its distribution in general narrows with increasing dome aspect ratio ($\sigma \approx 10\%$). The resultant microstructures on the two ends of the dome aspect ratio axis are shown in Figure 8c.

There are two additional observations made on the simulated microstructures. First, a small fraction of oxide was encapsulated within CoPt grains, which was also observed experimentally in another system.[11] Second, since the Ru grain size was initially set to be smaller than the dome pitch size, one dome may very likely consist of several Ru grains. When this happens, multiple CoPt grains grow on one dome due to the epitaxial relationship. This is also observed experimentally.[11]

Recalling the previous discussion on the interfacial energy terms, when the CoPt γ_{GB} was larger than γ_{CoPt/SiO_2}, the CoPt GBs became energetically favored for SiO_2 to occupy. Hence, the CoPt grain boundaries locally served as the "trapping" sites when SiO_2 diffused along the surface. Now that such diffusion occurred on a nonflat surface with certain curvature, with an extra chemical potential gradient introduced, according to Mullin's theory, to be added to the driving force of the surface diffusion in the direction from the dome top into the valley. The effect of this extra driving

DOI: 10.1021/acs.cgd.6b01248
Cryst. Growth Des. 2017, 17, 1016−1027

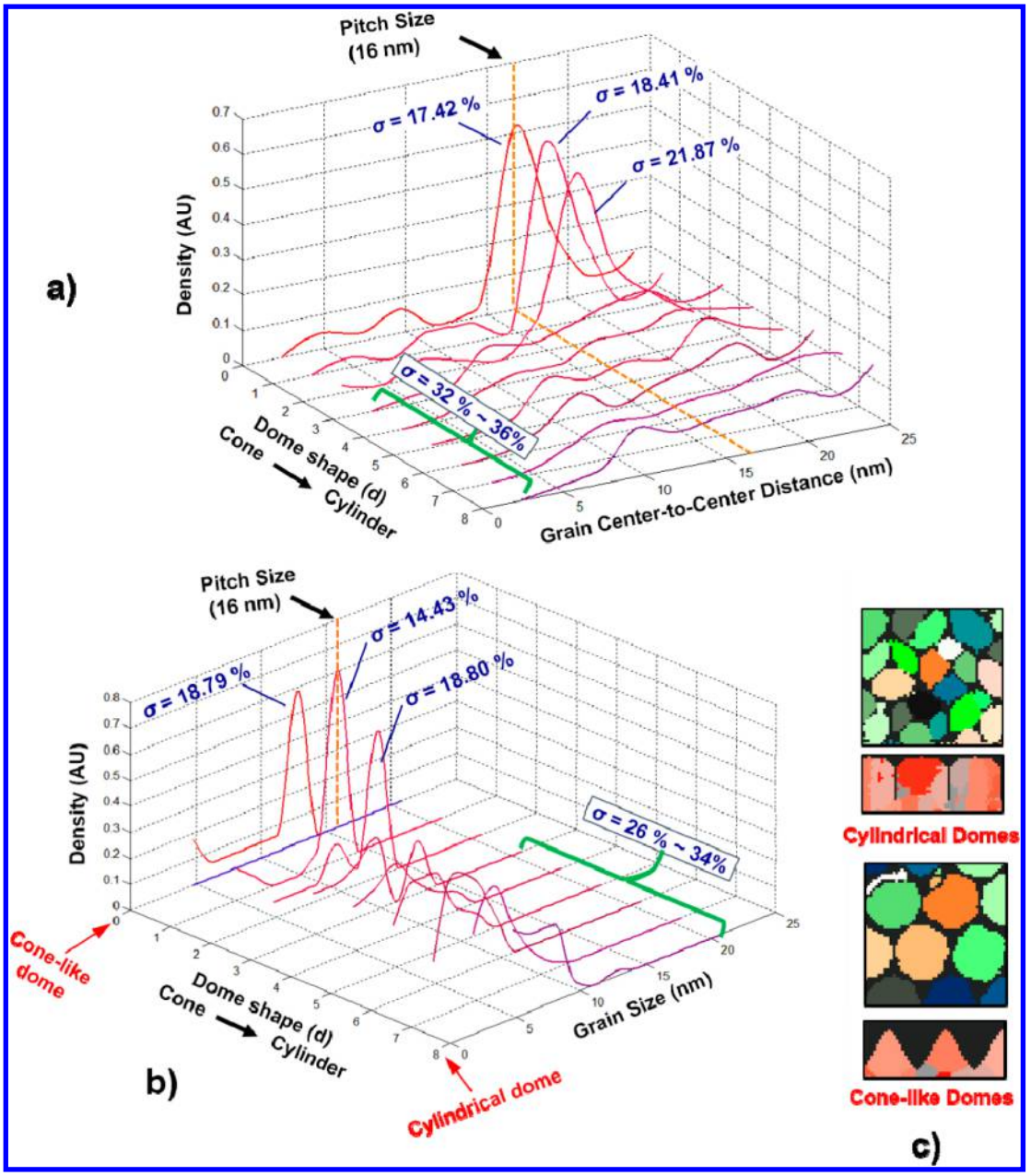

Figure 9. Effect of the dome shapes on the two-phase growth and the resultant microstructure: (a) grain center-to-center distance and its distribution σ. (b) Grain size and its distribution σ. (c) Plane view of as-simulated films with different dome shapes (shown below each plane view of domes).

force was fully manifested in the resultant microstructures as a function of the dome aspect ratio.

In the Low AR case, with very small curvature gradient of the domes, the effect of the curvature-introduced driving force was correspondingly weak, that other effects such as interfacial energy were more determinant in the microstructure formation. Therefore, with "trapping" sites existing along the diffusion path from the dome top into the valley, SiO_2 might experience local energy minimum at CoPt GBs. With small curvature-introduced driving force, it was less probable for SiO_2 to overcome the "trapping" sites of local energy minimum and would tend to stay in the CoPt GBs as shown in Figure 8b, the Low AR case. As a result, the average CoPt grain size was much smaller than the dome pitch size, with SiO_2 occupying not only the dome valley regions but also the CoPt grain boundaries across the domes. The grain size distribution in this case was large also due to the formation of multiple grains within the region of a single dome. Overall, the growth of the CoPt grains was not guided by the template with the dome aspect ratio being very small.

In the High AR case, with a sufficient curvature gradient, the effect of the curvature-introduced driving force dominated over interfacial energy, especially for the very first layers of voxels, that the "trapping" sites, or the local energy minimum, now could be overcome. This resulted in CoPt grains with an average size just slightly smaller than the dome pitch size (due to a finite SiO_2 segregant thickness) and an average grain center-to-center distance very close to the dome pitch size. The simulated microstructure in Figure 8b High AR case also clearly showed that the domes on the prefabricated template successfully guided the simultaneous two-phase growth of the CoPt grains and the SiO_2 segregant.

In addition, the coverage of the dome valley regions by SiO_2 was found to remain at a high level ~98%, even with very small

DOI: 10.1021/acs.cgd.6b01248
Cryst. Growth Des. 2017, 17, 1016−1027

dome aspect ratios. This could be explained by the fact that the valley region was maintained as energetically preferred sites by being the curvature maximum, and hence the total energy reduction would be the most when materials diffuse into the valley. Even though SiO_2 may experience local energy minimum during the diffusion process, the SiO_2 near the valleys would be able to fill them, while the SiO_2 far away from the valleys would be more likely to be trapped by the CoPt GBs that were energy minimum sites. This explains the case shown in Figure 1b in which the media film was grown on a substrate with Ru domes formed under high chamber pressure sputtering. Although we did not simulate the film growth in this particular case, using the understanding acquired in this study, it is reasonable to expect a complete coverage by SiO_2 segregant, and this would be the result of surface diffusion of the SiO_2 into the energy minima location in the valleys between the Ru domes formed by high-pressure sputtering. It should also be mentioned that there is limited control on the dome pitch size and its distribution for this type of Ru domes. In contrast, the dome pitch size and its distribution on the prefabricated template can be much better controlled.

3. Domes of Different Shapes. Another possible variation of the template topography is the dome shape, which can be manipulated during the ion milling process during fabrication. As stated in the discussion on the effect from the dome aspect ratio, the domes played a role in changing the surface energy gradient through their curvature gradient, or more specifically the chemical potential gradient, during the film growth. What is to be emphasized is that it is the curvature gradient that is important. In other words, the curvature maxima can remain the same while the profile of the curvature gradient changes. In the case of the changing dome aspect ratio, both the curvature maxima and the curvature gradient changed. However, the curvature maxima do not necessarily have to be changed in order for the curvature gradient to change. This is the case presented in Figure 9 that when the dome shape changes, the resultant microstructure changes with the changing curvature gradient.

As shown in Figure 9a, when the dome changes from a cone shape to a cylinder, the curvature gradient changed without changing the curvature maxima at the dome tops and valleys; however the guided two-phase growth effect from the template vanished. This is apparently caused by the flattened curvature gradient from dome top into the valley. The same results can be seen from Figure 9b for the CoPt grain size and its distribution (σ increased from 14% to 19% with cone-shaped domes to 26−34% with cylindrical domes).

However, one difference noticed in the case compared to the aspect ratio simulation was the coverage of valley region, which changed drastically when the dome shape changed. It was obvious that for cylindrical domes, valleys were narrower compared to a more open valley for cone-like domes. Thus, in order to fully occupy the valley, SiO_2 should not only overcome the local energy minima created by GBs during lateral surface diffusion, but also needs to diffuse vertically through a narrow channel between the domes without any chemical potential gradient within. Therefore, it was much less likely for SiO_2 to completely fill the valleys of such a template with neighboring cylindrical domes, rendering a media film that cannot function properly.

If the curvature on the domes is carefully designed, the curvature gradient profile can also change with neither aspect ratio nor dome shape being changed.

Even though the dome shape would not influence the specific curvature within the valleys, the resultant microstructure revealed that the percentage of the valleys being filled would still vary greatly with the changing dome shape. This means that the curvature gradient was dominant in controlling SiO_2 to fill the valley by changing the surface energy gradient. In addition, with the presence of energy minima caused by CoPt GBs, the probability of SiO_2 not being "trapped" inside GBs depended on the driving force of surface energy gradient as shown in Figure 8 and Figure 9. Therefore, it could be concluded that the surface energy gradient induced by the prefabricated template dominated the surface diffusion of mobile species through the growth of the film, resulting in a highly ordered microstructure similar to the experimental one shown in Figure 1c, or the simulated one in Figure 10c.

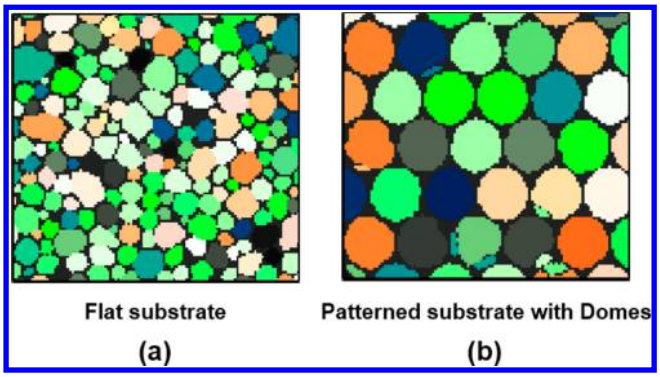

Figure 10. Plane view of CoPt/SiO_2 film growth on polycrystalline Ru substrate with different topographies: (a) flat substrate (b) patterned substrate with cone-like domes with aspect ratio (AR) = 0.8.

The simulation results presented thus far have covered a variety of factors that influence the resultant thin film microstructure. Some aspects regarding the fundamental mechanism have been briefly discussed. Through these results and discussion, it has been identified that the key to a successful templated two-phase growth is the surface diffusion process, of which there are two aspects that need to be taken into account: a thermodynamic point of view and a kinetic one.

The thermodynamics considerations on the driving force of the surface diffusion in the two-phase growth include two aspects: the interfacial energy minimization and the surface energy gradient due to the curvature gradient of a nonflat substrate. The former concerns mainly the interfacial energies between species and the magnitude of the latter depends on both surface energy of the materials and the surface curvature. The kinetic consideration on the other hand mainly concerns the mobility of the materials. In this model, the mobility relates to the surface energy of the materials and the bonding energy between the different species. Potentially, the deposition temperature of the film that relates to the simulation parameter "lattice temperature" can also affect the film microstructure. This was not explored in this study since the deposition of CoPt−SiO_2 films were carried out at room temperature experimentally. From a practical point of view, the thermodynamic as well as the kinetic considerations in fact translate into materials selection that determines all the energy-related terms and the dome geometry that must be well-controlled for a successful two-phase growth process.

From the simulations, we also conclude that during an effective two-phase growth process (up to 8−10 nm film thickness), there

DOI: 10.1021/acs.cgd.6b01248
Cryst. Growth Des. 2017, 17, 1016−1027

is a transition of dominant mechanism. During the very early stages of film growth, i.e., the first couple of voxel layers, if the curvature gradient is sufficiently large and it is the dominant parameter defining the chemical potential gradient, it therefore dominates the driving force of the surface diffusion. Given proper interfacial energy ratios, the oxide will go to the valley between the domes, while the CoPt grains grow epitaxially on the dome tops. As the film grows thicker, the curvature reduces continuously, the new materials arriving on the film surface now see much less chemical potential gradient introduced by curvature than that during the very early stage of film growth. Therefore, the interfacial energy gradually takes over as the dominant mechanism. In other words, if the desired film microstructure can be established early on with the appropriate materials and domes, the later grown film will most likely follow this microstructure regardless. In principle, this conclusion could be potentially verified via experimental work through a series of characterizations of the film sputtered at different thicknesses, using transmission electron microscopy (TEM), or even in situ TEM, and though challenging to do, such experimental verification of the proposed mechanism is still worth considering for future work.

Since this hybrid simulation model was developed based on the Potts model MC method, the limitations from Potts model were inherited. One limitation would be the discretization issue. Trials were made for this hybrid model using different discretization grids, and the voxel size could not be finer than a certain limit, beyond which artificial cubic anisotropy could be introduced while the atomic structure of the material did not have cubic symmetry. Another minor limitation might be the scaling of time. Usually, the scaling of real time and simulation time of grain growth process for Potts model could be achieved by scaling of the grain growth rate in simulation with the experimental growth rate. However, in this model, the diffusion of materials took place while the diffusivity of each component could hardly be estimated systematically. Therefore, the simulation time could not be scaled with respect to the real time in this model. On the basis of the above-mentioned limitations, molecular dynamics (MD) might be a more suitable method for further investigation with quantitative accuracy on this templated film growth process. However, it could be expected that a MD study of this templated growth process on the scale of interest, for instance, 100 nm wide, would require an extraordinary amount of computational resource and time. The developed hybrid model, on the other hand, was a fairly well balanced compromise between simulation time and the physical size of the system to be simulated. On the basis of MC, this model was computational efficient, and it was sufficiently instructive on the understanding of the dominant mechanism of the concerned film growth.

SUMMARY

(1) A hybrid model, combining the scanning surface Potts model MC and level set method was developed and was used to study the effect from the templated substrate on the simultaneous growth of the two phases of the composite CoPt−SiO_2 film.

(2) Through conventional Potts model MC simulations, the relation between different interfacial energies and the rate of different events was analyzed, and the roles they played in microstructure formation were also evaluated. They were found to greatly influence the resultant film microstructure.

(3) For the template to properly guide the two-phase growth into the desirable microstructure, the driving force of the surface lateral diffusion must be the surface energy gradient that has been sufficiently modified by the nonflat features of the template. This can be achieved by either the dome features having a sufficiently high aspect ratio or having a cone-like shape.

(4) It was also found that the surface energy gradient driven surface lateral diffusion was the dominant mechanism in the early stage of deposition, but later transitioned into the interfacial energy dominated lateral diffusion in the later stage. The key to a successful templated two-phase film growth is to control the surface energy gradient through the optimized template features.

ASSOCIATED CONTENT

Supporting Information

The Supporting Information is available free of charge on the ACS Publications website at DOI: 10.1021/acs.cgd.6b01248.

Details of determination of activation energy for diffusion, determination of the relative ratio of $\gamma_{CoPt/SiO_2}/\gamma_{epi}$ and the detail of diffusion behavior for CoPt and SiO_2 in templated growth (PDF)

AUTHOR INFORMATION

Corresponding Author

*Address: Sun Yat-sen University, No. 132, Waihuan Dong Road, Guangzhou, Guangdong, 510006 P.R. China. Phone: 86-20-39943462 Email: zhjingxi@mail.sysu.edu.cn. Website: http://thematerialsgroupatjie.weebly.com/.

ORCID

Xiao Lu: 0000-0002-3883-3812

Jingxi Zhu: 0000-0002-0019-0647

Notes

The authors declare no competing financial interest.

ACKNOWLEDGMENTS

The authors would like to acknowledge the use of Parallel Grain Growth programs developed in the Department of Materials Science and Engineering at Carnegie Mellon University. Also, the National Science Foundation of China, Guangdong Province, Project Fund No. 2015A030310281 is acknowledged, along with the SYSU-CMU JRI Project Fund No. 20140307. The authors would like to thank Professors Anthony Rollett and Elizabeth Holm of the Department of Materials Science and Engineering at Carnegie Mellon University for helpful discussions. The author would also like to thank Brian Lin and William Fraizer, former graduate students of the Department of Materials Science and Engineering at Carnegie Mellon University, for the help in the programs.

REFERENCES

(1) Sundar, V.; Zhu, J.; Laughlin, D. E.; Zhu, J.-G. (Jimmy). Novel Scheme for Producing Nanoscale Uniform Grains Based on Templated Two-Phase Growth. *Nano Lett.* **2014**, *14*, 1609.

(2) Park, S. H.; Kim, S. O.; Lee, T. D.; Oh, H. S.; Kim, Y. S.; Park, N. Y.; Hong, D. H. Effect of top Ru deposition pressure on magnetic and microstructural properties of CoCrPt-SiO media in two-step Ru layer. *J. Appl. Phys.* **2006**, *99*, 08E701.

(3) Piramanayagam, S. N.; Pock, C. K.; Lu, L.; Ong, C. Y.; Shi, J. Z.; Mah, C. S. Grain Size reduction in CoCrPt:SiO_2 perpendicular recording media with oxide-based intermediate layers. *Appl. Phys. Lett.* **2006**, *89*, 162504.

(4) Srinivasan, K.; Wong, S. K.; Piramanayagam, S. N.; Kay, Y. S. Influence of synthetic nucleation layers on the microstructure, magnetic

DOI: 10.1021/acs.cgd.6b01248
Cryst. Growth Des. 2017, 17, 1016−1027

properties, and recording performance of CoCrPt-SiO_2 perpendicular recording media. *J. Appl. Phys.* **2008**, *103*, 093912.
(5) Tham, K. K.; Hinata, S.; Saito, S.; Takahashi, M. Metal-oxide buffer layer for maintaining topological bumpy surface underlayer of columnar CoPt-SiO_2 granular media deposited at high substrate temperature. *J. Appl. Phys.* **2015**, *117*, 17A923.
(6) Jensen, P. Growth of nanostructures by cluster deposition: Experiments and simple models. *Rev. Mod. Phys.* **1999**, *71* (5), 1695.
(7) Wang, Y.; Ely, D. R.; García, R. E. Progress Towards Modeling Microstructure Evolution in Polycrystalline Films for Solar Cell Applications, IEEE 39th Photovoltaic Specialists Conference (PVSC). Tampa Convention Center, Tampa, FL, United States, June 16−21, 2013, 2056.
(8) Sun, Y.; Caflisch, R.; Engquist, B. Multiscale Method for Epitaxial Growth. *Multiscale Model. Simul.* **2011**, *9* (1), 335.
(9) Lee, H.-S.; Guo, V.; Zhu, J.-G.; Laughlin, D. E. Control of resputtering in biased CoCrPt-SiO_2 media to enhance grain decoupling and grain size distribution. *J. Appl. Phys.* **2008**, *103*, 07F541.
(10) Zhu, J.-G.; Peng, Y.; Laughlin, D. E. Toward an understanding of grain-to-grain anisotropy field variation in thin film media. *IEEE Trans. Magn.* **2005**, *41* (2), 543.
(11) Sundar, V. Templated Two-phase Growth of Magnetic Recording Media. Ph.D. thesis. Carnegie Mellon University, Pittsburgh, 2014.
(12) Francis, A. J.; Roberts, C. G.; Cao, Y.; Rollett, A. D.; Salvador, P. A. Monte Carlo simulations and experimental observations of templated grain growth in thin platinum films. *Acta Mater.* **2007**, *55*, 6159.
(13) Li, D. Y.; Szpunar, J. A. A Monte Carlo simulation approach to the texture formation during electrodeposition-I. The simulation model. *Electrochim. Acta* **1997**, *42* (1), 37.
(14) Potts, R. B. Some Generalized Order-Disorder Transformations. *Math. Proc. Cambridge Philos. Soc.* **1952**, *48* (1), 106.
(15) Ising, E. Beitrag zur Theorie des Ferromagnetismus. *Z. Phys.* **1925**, *31* (1), 253.
(16) Metropolis, N.; Rosenbluth, A. W.; Rosenbluth, M. N.; Teller, A. T.; Teller, E. J. Equation of State Calculations by Fast Computing Machines. *J. Chem. Phys.* **1953**, *21*, 1087.
(17) Huang, J. C. A.; Hsu, A. C.; Lee, Y. H.; Wu, T. H.; Lee, C. H. Influence of Crystal Structure on the Perpendicular Magnetic Anisotropy of an Epitaxial CoPt alloy. *J. Appl. Phys.* **1999**, *85* (8), 5977.
(18) Radhakrishnan, B.; Zacharia, T. The Effect of Lattice Temperature on Abnormal Subgrain Growth Simulations using a Monte Carlo Technique. *Interface Sci.* **2002**, *10*, 171.
(19) Gleiter, H. Theory of grain boundary migration rate. *Acta Metall.* **1969**, *17*, 853.
(20) McDowell, H. K.; Doll, J. D. Theoretical Studies of surface diffusion: Self-diffusion in the BCC (110) System. *Surf. Sci.* **1982**, *121* (1), L537.
(21) Voter, A. F.; Doll, J. D. Transition State Theory Description of Surface Self-diffusion: Comparison with Classical Trajectory Results. *J. Chem. Phys.* **1984**, *80*, 5832.
(22) Truhlar, D. G.; Garrett, B. C.; Klippenstein, S. J. Current Status of Transition-State Theory. *J. Phys. Chem.* **1996**, *100*, 12771.
(23) Sethian, J. A. *Level Set Methods and Fast March Methods Evolving Interfaces in Computer Geometry, Fluid Mechanics, Computer Vision, and Material Science*; Cambridge University Press: New York, 2005; part IV, Chapter 5.2.
(24) Osher, S.; Fedkiw, R. P. Level Set Methods: An Overview and Some Recent Results. *J. Comput. Phys.* **2001**, *169* (2), 463.
(25) Adalsteinsson, D.; Sethian, J. A. A Level Set Approach to a Unified Model for Etching. Deposition. And Lithography I: Algorithms and Two Dimensional Simulations. *J. Comput. Phys.* **1995**, *120* (1), 128.
(26) Osher, S.; Sethian, J. A. Fronts Propagating with Curvature Dependent Speed: Algorithms Based on Hamilton-Jacobi Formulations. *J. Comput. Phys.* **1988**, *79*, 12.
(27) Osher, S.; Fedkiw, R. *Level Set Methods and Dynamic Implicit Surfaces*, 1st ed. Cambridge University Press: New York, 2003; p 25.
(28) Adalsteinsson, D.; Sethian, J. A. A Level Set Approach to a Unified Model for Etching. Deposition. And Lithography II: Three dimensional simulations. *J. Comput. Phys.* **1995**, *122*, 348.
(29) Lai, B. *Simulation of Perpendicular Media Deposition Using Level Set Method*. Master Thesis, Sun Yat-sen University, June 2015.
(30) Chen, Q.; Chang, C.; Lee, L.; Harkness, S. D. Inter layers for perpendicular recording media US 7235314 B2, June 26, 2007.
(31) Zheng, Y. G.; Lu, C.; Mai, Y.-W.; Gu, Y. X.; Zhang, H. W.; Chen, Z. Monte Carlo simulation of grain growth in two-phase nanocrystalline materials. *Appl. Phys. Lett.* **2006**, *88*, 144103.
(32) Zheng, Y. G.; Lu, C.; Mai, Y. − W.; Zhang, H. W.; Chen, Z. Model-Based Simulation of Normal Grain Growth in a Two-Phase nano-structured system. *Sci. Technol. Adv. Mater.* **2006**, *7*, 812.
(33) Dannenberg, A.; Gruner, M. E.; Hucht, A.; Entel, P. Surface energies of stoichiometric FePt and CoPt alloys and their implications for nanoparticle morphologies. *Phys. Rev. B: Condens. Matter Mater. Phys.* **2009**, *80*, 245438.
(34) Andreazza, P.; Pierron-Bohnes, V.; Tournus, F.; Andreazza-Vignolle, C.; Dupuis, V. Structure and order in cobalt/platinum-type nanoalloys: from thin films to supported clusters. *Surf. Sci. Rep.* **2015**, *70*, 188.
(35) Kumikov, V. K.; Khokonov, Kh. B. On the Measurement of Surface Free Energy and Surface Tension of Solid Metals. *J. Appl. Phys.* **1983**, *54*, 1346.
(36) Galanakis, I.; Papanikolaou, N.; Dederichs, P. H. Applicability of the Broken-Bond Rule to the Surface Energy of the FCC Metals. *Surf. Sci.* **2002**, *511* (Issues 1−3), 1.
(37) Shchipalov, Y. K. Surface Energy of Crystalline and Vitreous Silica. *Glass Ceram.* **2000**, *57* (11/12), 374.
(38) Mullins, W. W. Mass transport at interface in single component systems. *Metall. Mater. Trans. A* **1995**, *26* (8), 1917.

DOI: 10.1021/acs.cgd.6b01248
Cryst. Growth Des. 2017, 17, 1016−1027